Journal of Applied Fluid Mechanics, Vol. 11, No. 2, pp. 475-481, 2018.
Available online at www.jafmonline.net, ISSN 1735-3572, EISSN 1735-3645.
DOI: 10.29252/jafm.11.02.27936

Evaluating the Effects of Blade Tip Clearance in Various Stages on the Performance of an Axial Compressor

M. Ostad and R. Kamali†

Department of Mechanical Engineering, Shiraz University, Shiraz, Iran.

†*Corresponding Author Email: rkamali@shirazu.ac.ir*

(Received May 1, 2017; accepted November 6, 2017)

ABSTRACT

In the current study, the influence of blade tip clearance in different stages of a three-stage compressor is investigated. Performance diagrams of compressor were verified against experiment when there is no change in the tip clearance, after which the effect of tip clearance for the cases, 1, 1.5 and 2 mm, in the first, second and third stages of rotor was studied. The results indicated that the impact of tip clearance increase did not have any effect on choked flow rate value in the first and second stages, and only the change in the third stage tip clearance reduced the choked flow rate. For the same tip clearance value, the highest compressor performance loss occurs in the case of applying the tip clearance in the third stage, which is also the final stage and is highly sensitive to tip clearance changes. Moreover, modifying the tip clearance is effective on the flow angle in the trailing edge and as the tip clearance increases, the same thing happens about the flow angle. The maximum value of flow angle changes by modifying the tip clearance belongs to the third stage of the compressor.

Keywords: Variable tip clearance; Stall margin; Flow angle; Compressor performance.

NOMENCLATURE

g	gravity
h	enthalpy
P	pressure
Pr	pressure ratio
Re	Reynolds number
T	temperature
Y^+	none dimensional normal distance to wall
η	isentropic efficiency
ρ	density
ω	angular velocity

1. INTRODUCTION

Compressors are always mentioned as the heart of gas turbines and define the performance characteristics and overall system instability. The existence of adverse pressure gradient in the compressor increases its sensitivity to flow thermodynamic changes and geometry aerodynamics and the more this adverse pressure gradient, the more the sensitivity to these changes. The flow in the tip clearance has an important effect on the overall efficiency and compressor stability. Various methods such as application of casing treatment (Kim *et al*. 2013), swept and leaned blades, using winglet on the suction side (Zhong *et al*. 2011), and utilizing vertical impact jet (Bae *et al*. 2003) have been proposed to control the tip clearance flow and to achieve better stability and overall efficiency of the compressor. In general, tip clearance distance is unavoidable and always due to manufacturing limitations exist. The existence of two fundamental problems, namely, the reduction of output work and compressor efficiency is the reason that researchers have tried to minimize the tip clearance loss in the past 60 years. In recent years, many researches have been conducted on the tip clearance loss. Danisha *et al*. studied the tip clearance loss in a multi-stage compressor and noticed that an increase in the tip clearance, results in compressor performance loss in addition to pressure ratio and efficiency. Furthermore, the tip clearance value is effective on the choked flow rate and the more the tip clearance, the less the choked flow rate (Danisha *et al*. 2016). An study on the tip clearance conducted by Ramakrishna and Govardhan in swept blades showed that the effect of tip clearance is much more in swept blades than in blades lacking any swept (Ramakrishna *et al*. 2009). The inspection of blade tip clearance in transonic compressor reveals that the tip gap chokes

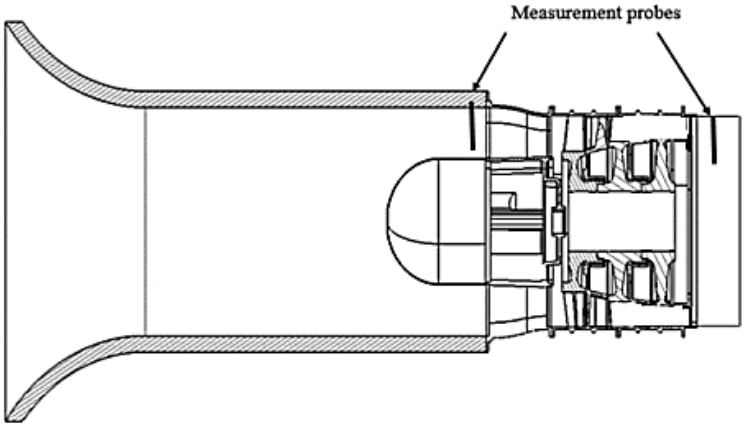

Fig. 1. Cross section of investigated compressor.

the flow near the wall and it increases downstream, and because of the interaction between vortices resulted from the tip gap and the main flow, the flow rate decreases (Ren *et al*. 2016). Researches done by Cumpsty showed that for each 1% increase in tip clearance over 6% increase in the blade chord, the pressure and the flow coefficient increase by, respectively, 23% and 15% (Storer *et al*. 1994). Denton has cited the tip clearance loss as the main loss source in compressors (Denton 1993). The tip clearance in compressor's instable conditions, especially close to stall state, creates more sensitivity and causes more flow be chocked. Moreover, blade tip flow plays an important role in the stability of the compressor (Yamada *et al*. 2007; Day 1993; Vo *et al*. 2008). Bajoie Liou *et al*. empirically studied the effect of tip clearance on 3-D flow separation in rotor and choking flow and could find out that under certain conditions, flow separation from stator's blade leading edge in the hub section, results in flow separation and instability of compressor stage (Liou *et al*. 2016). When stall occurs, flow separation starts off from the rotor blade tip proximity (Day 2015). Some specific features of blade tip flow can be considered as stall criteria. After the conducted investigations (Day 1997; He 1997; Hah *et al*. 2006), there are three features that can be predominated in propeling to stall condition. The first property is, when the slope of total pressure rise to static pressure of compressor becomes negative. The second property, is the interface between the blade tip clearance and domain flow in compressor, which has become parallel to the leading edge of compressor. The third property, is the start of backflow at the trailing edge of the compressor near the blade tip region. The conducted studies generally focused on one geometry including rotor and stator and usually considered the blade tip clearance in an isolated geometry. In this article, we try to evaluate the effect of the same blade tip clearance on various stages of a three-stage compressor, then discuss different parameters having an effect on the flow.

2. TEST SECTION

The mentioned compressor is composed of three rotor and stator stages plus one inlet guide vane for which the geometrical properties are mentioned in Table 1. Fig. 1 clearly shows that for the flow to uniformly enter the compressor, the Bellmouth geometry was designed at intake and pressure and temperature probe were placed at the beginning and at the end of compressor. The results of this compressor were obtained at its nominal rotational velocity, 28015 rpm. Fig. 2 shows the settlement of probe at the intake.

Table 1 Specification of investigated compressor

Compressor	Number
IGV Blade	3
First rotor blades	23
First stator blades	49
Second rotor blades	27
Second stator blades	47
Third rotor blades	31
Third stator blades	47

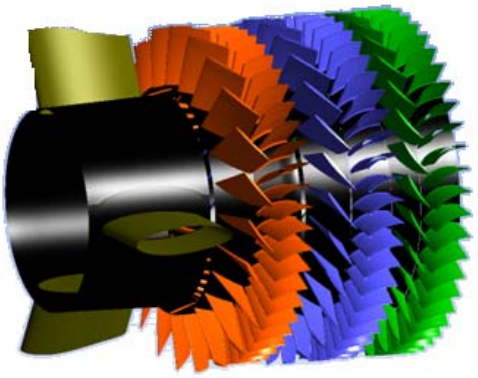

Fig. 2. Compressor's computational domain.

The output results of temperature and stagnation pressure are related to the inlet guide vane, (IGV) at the flow inlet and the compressor outlet.

Fig. 3. A view of tested compressor.

3. MESH GENERATION

To fliud analysis in the compressor, the 3-D geometrical model of the compressor was created beforehand. Therefore, considering the provided facilities and modeling conditions, attempts were made to apply the best grid on this model. After creating the desired 3-D geometry, TURBOGRID was utilized to generate to apply a computational grid, using The ATM Optimized, which is a method for creating a mesh. It enables you to control the global mesh size as well as the mesh size at the boundary layer، topology and boundary layer configurations. Since the effects of boundary layer were observed, the circumferential mesh was made small and a value of 30 was considered for the associated y^+. Due to the limited value of y^+, the quality of the selected grid was increased to excel the turbulence modeling in the boundary layer.

$$\Delta y = L\Delta y^{+}\sqrt{80}\, Re_x^{\frac{1}{14}} \frac{1}{Re_L} \quad (1)$$

The value of y^+ is determined using Eq. (1). This mesh was created considering the $y^+ < 30$ condition in order for utilizing the appropriate turbulence model so that satisfactory compatibility is achieved with the turbulence model in use. Each computational domain Reynolds number in the above equation, was obtained from the velocity of flow curve solution. Fig. 4 shows the computational grid sample. It can be seen that the grid for all sections was created using the hexahedral mesh technic.

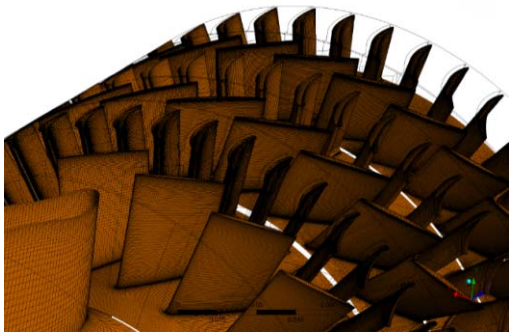

Fig. 4. Computational grid sample.

4. NUMERICAL ANALYSIS

The solved equations in this turbulence model included the following equations:

Conservation of mass:

$$\partial\rho/\partial t+\vec{\nabla}\cdot(\rho\vec{v}) = 0 \quad (2)$$

Conservation of momentum:

$$\rho\partial\vec{v}/\partial t+ \rho\cdot(\vec{v}\cdot\nabla)\,\vec{v}=\nabla p+\nabla\tau+\rho\vec{g} \quad (3)$$

Conservation of energy:

$$\partial(\rho h_{tot})/\,\partial t \;-\; \partial p/\partial t \;+\; \nabla\cdot(\,\rho U h_{tot})= \nabla\cdot(\lambda\,\nabla T) \;+\; \nabla\cdot(U\cdot\tau) + U\cdot S_M + S_E \quad (4)$$

$$h_{tot}=h+\frac{1}{2}U^2 \quad (5)$$

Where h_{tot} is the total enthalpy and a function of pressure and temperature. The term $\nabla\cdot(U\cdot\tau)$ represents the work done by stresses due to viscosity. This term is the source of internal heat because of fluid viscosity which can be neglected in most flows. $U\cdot S_M$ is the term describing the momentum from external sources which is also negligible. To numerically analyze the effect of tip clearance on the performance of the blade, K-Epsilon RNG turbulence model was used. This has the advantage of better prediction where the flow separation occurs and how the compressor acts. For some special cases, one-equation Spalart Allmaras turbulence model was used for the modeling purpose (Kim *et al*. 2013) which presents a weaker prediction than K-Epsilon RNG turbulence model. The equation form of K-Epsilon RNG turbulence method is as follows:

$$\partial(\rho k)/\,\partial t+\partial/\partial x_i(\rho k u_i)= \partial/\partial x_j[(\alpha_k\mu_{eff})(\,\partial k/\,\partial x_j)]+G_k +G_b-\rho\varepsilon-Y_M+S_k \quad (6)$$

$$\partial(\rho\varepsilon)/\,\partial t+\partial/\,\partial x_i(\rho\varepsilon u_i)= \partial/\partial x_j[(\alpha_\varepsilon\mu_{eff})(\,\partial\varepsilon/\partial x_j)]+C_{1\varepsilon} (\varepsilon/k)(G_k+C_{3\varepsilon}G_b)-(C_{2\varepsilon}\rho\varepsilon^2)/k-R_\varepsilon+S_\varepsilon \quad (7)$$

In these equations, μ_{eff} is defined as the sum of turbulence and molecular viscosity. G_b and G_k are the k production value due to buoyancy and average velocity gradient. The term Y_M shows the compressible turbulent flow expansion distribution relative to total dissipation rate. The terms $C_{1\varepsilon}$, $C_{2\varepsilon}$ and $C_{3\varepsilon}$ are constant coefficients and α_k and α_ε are the reverse of effective Prandtl numbers of turbulent flow kinetic energy and dissipation rate. The boundary conditions at the compressor inlet include stagnation pressure and temperature taken as 0.884 bar and 284 K, respectively. The physical time scale was used that it is calculated by (1/ω) which ω is angular velocity. One passage in each stage was used and the periodic interface between blades in a stage was exerted. The interface between rotor and stator is stage condition, the stage model performs a circumferential averaging of the fluxes through bands on the interface. Compressor performance diagrams were progressively obtained by application of variable static pressure at the compressor outlet.

5. MESH INDEPENDENCY

To make sure the obtained results are independent of the grid, four kinds of grid were applied on the geometry and the results were compared according to pressure ratio and efficiency after which the value of 5862452 was determined as the optimal estimation for the considered grid.

Table 2 Mesh independency

Mesh element	Efficiency	Total pressure ratio
2706639	0.51544	1.79
3909277	0.52542	1.814
5862452	0.5304	1.823
6320254	0.5306	1.822

$$\mathrm{Pr} = P_{total\ out}/P_{total\ in} \tag{8}$$

$$\square_{\mathrm{tot}} = \frac{((P_{out}/P_{in})^{(\frac{\gamma-1}{\gamma})}-1)}{T_{out}/T_{in}} \tag{9}$$

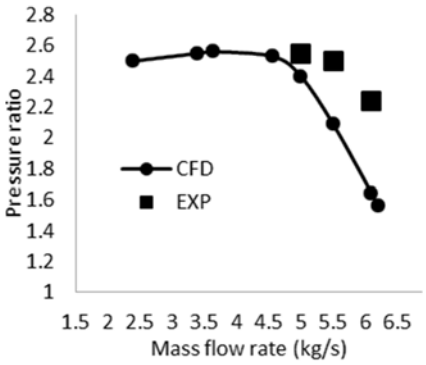

Fig. 5. Pressure ratio vs inlet mass flow rate in the compressor.

6. COMPARSION NUMERICAL AND EXPERIMENTAL DATA

The results of numerical simulation were compared with the experimental data as a comparison step, depicted in Figs. 5 and 6. As previously mentioned, the comparison for the numerical and experimental results was achieved at a rotational speed of 28015 rpm. The maximum computational difference is equal to 8% in the operating condition and there is a good agreement between the obtained pressure diagram from the numerical simulation and the experimental data.

Figure 6 shows the numerical and experimental results related to total isentropic efficiency from Eq. (9). It is obvious that the numerical data closely follow the experimental ones.

7. IMPACT OF TIP CLEARANCE AT VARIOUS ROTORS

It is obvious that the numerical data closely follow the experimental ones. The impact of various tip clearances for three cases of 1, 1.5 and 2 mm in the first, second, and third stages of the compressor's rotors were studied and performance charts were attained for all three cases. The performance diagrams of the compressor shown in Fig. 7 are an indication that the tip clearance effect is much more considerable in the third rotor than the first and second rotors. The effect of 1 mm tip clearance in all three stages on stall margin is different and the third stage rotor takes the most impression from the tip clearance change and the stall margin significantly drops for this case, Fig. 8. Figs. 9-12 show that as the tip clearance of the third stage increases, choked flow rate decreases whereas this increase does not have any effect on the choked flow rate of the first and second stages, since the flow rate is always determined by the final compressor stage. The diagrams depicting various tip clearances height cases indicate that tip gap shows its effect for the near-stall condition and plays a significant role in the compressor stability. by increasing adverse gradient pressure in the compressor, the flow separation has happened at the tip gap and then due to the tip clearance flow has not the adequate kinetic energy to overcome the adverse pressure gradient, it would be stopped tip clearance fluid from further moving in the compressor and this condition provides the stall of compressor.

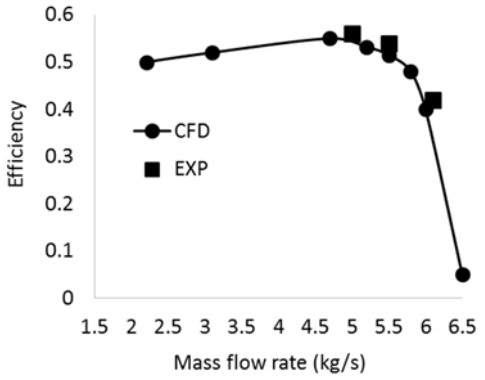

Fig. 6. Total isentropic efficiency vs inlet mass flow rate in the compressor.

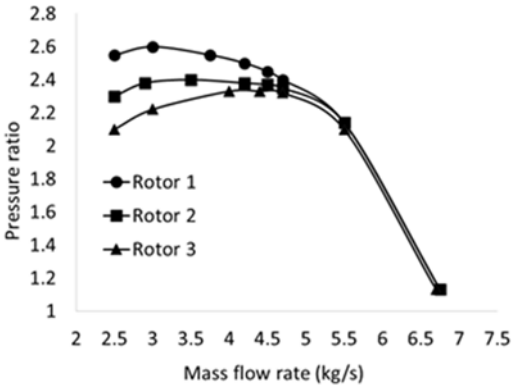

Fig. 7. The effect of 1 mm tip clearance in various rotors on pressure ratio of the compressor.

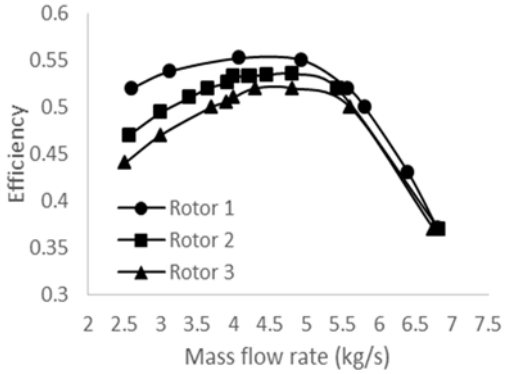

Fig. 8. Effect of 1 mm tip clearance in various stages on isentropic efficiency of the compressor

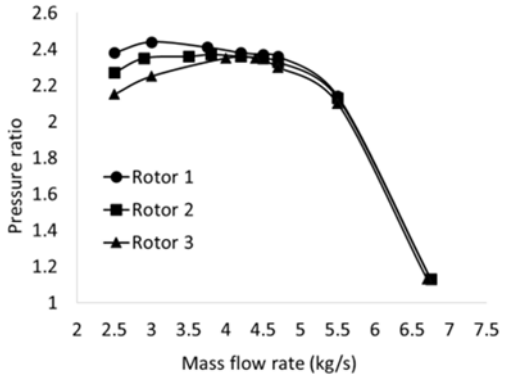

Fig. 9. Effect of 1.5 mm tip clearance in various stages on pressure ratio of the compressor.

Figure 10 shows the compressor efficiency changes for the case when the tip clearance is 1.5 mm. As can be seen, the slope of third stage rotor shows a faster reduction rate. As the isentropic efficiency is dependent on two variables, namely, temperature and pressure, tip clearance gap height was increased from 1 mm to 1.5 mm not only decreases the pressure ratio but also effects the outlet to inlet temperature ratio of the compressor and these two factors make the tip clearance effect to be more dominant on the isentropic efficiency than the stage pressure.

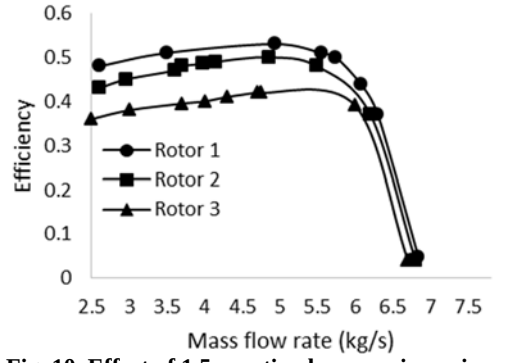

Fig. 10. Effect of 1.5 mm tip clearance in various stages on isentropic efficiency of the compressor.

Figure 11 shows the effect of 2 mm tip clearance on the rotors of first, second and third stages. The applied tip clearance in the third stage had a 0.18 kg/s effect on the choked flow rate. The 2 mm tip gap was more effective on the third stage rotor and the pressure curve of this case, approaches the compressor surge conditions with a higher slope.

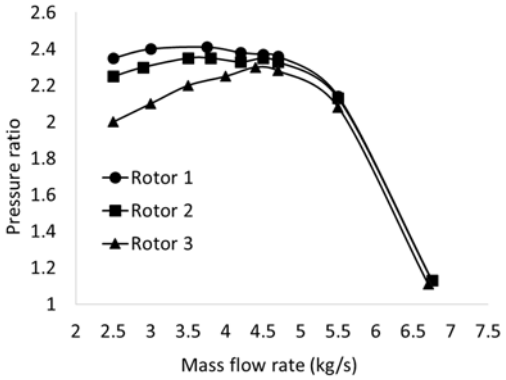

Fig. 11. Effect of 2 mm tip clearance in various stages on pressure ratio of the compressor.

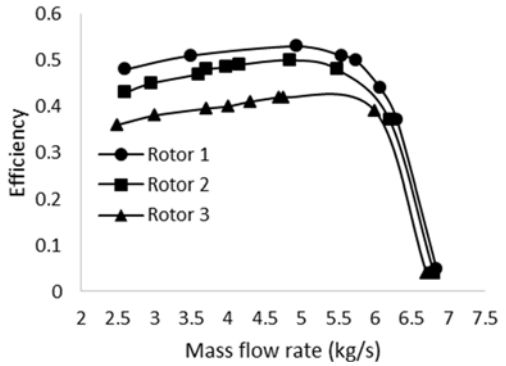

Fig. 12. Effect of 2 mm tip clearance in various stages on isentropic efficiency of the compressor.

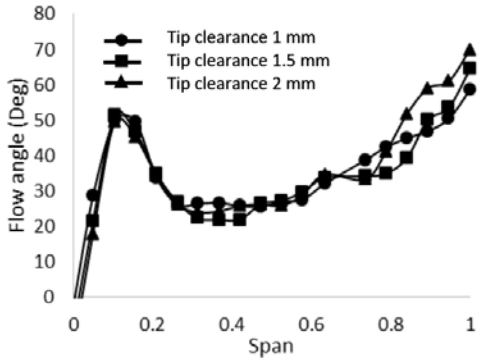

Fig. 13. Effect of tip clearance on outlet flow angle of first rotor.

As can be noticed from Fig. 13, the increase in tip clearance is effective on the outlet flow angle. The biggest value of this angle change happened in third stage for a tip clearance of 2 mm, Fig. 15. This angle change in the flow takes place in the final 20% of rotor span and for other points along the rotor span, no considerable effect is seen.

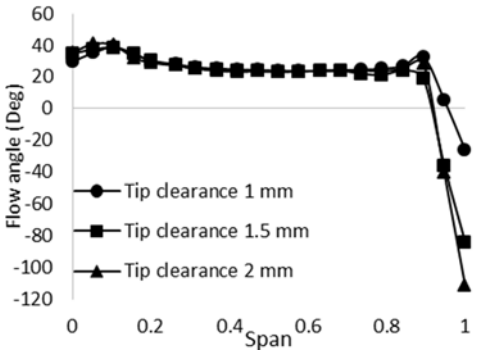

Fig. 14. Effect of tip clearance on outlet flow angle of second rotor.

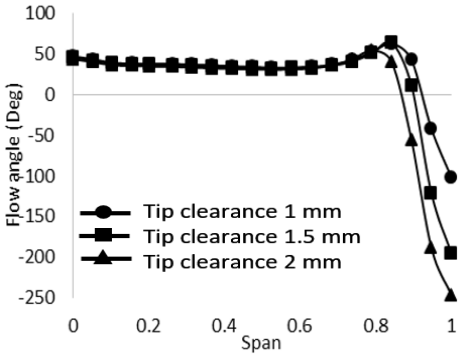

Fig. 15. Effect of tip clearance on outlet flow angle of third rotor.

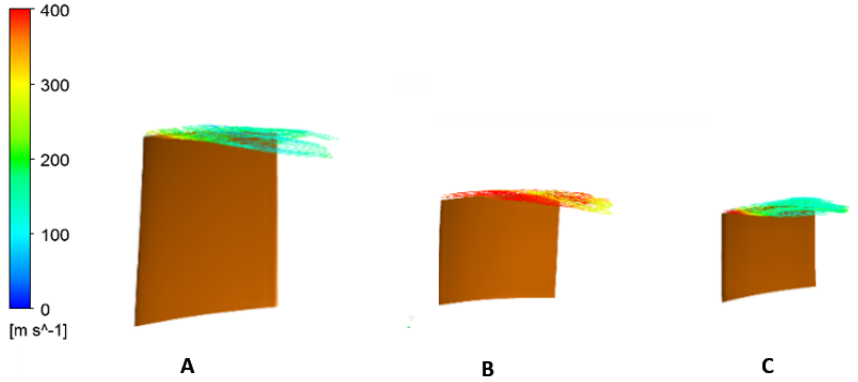

Fig. 16. Leaked flow from the tip gap in the A) first stage rotor B) second stage rotor C) third stage rotor.

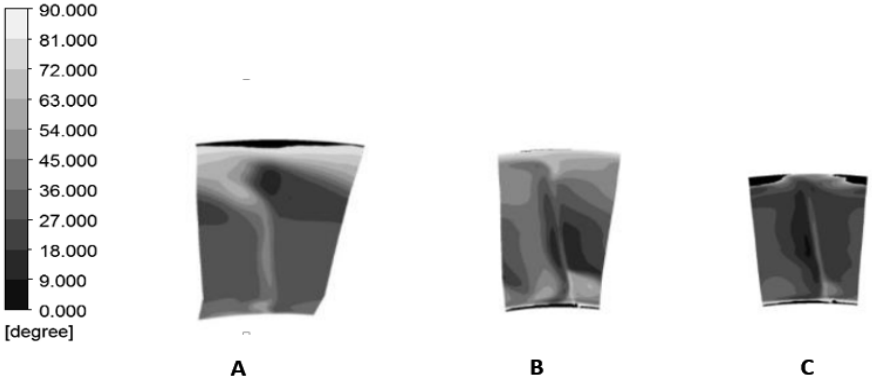

Fig. 17. Outlet flow angle from the A) first stage rotor B) second stage rotor C) third stage rotor.

Also noticed from Fig. 13 is the fact that for tip clearance changes from 1 to 2 mm, the outlet flow angle from the trailing edge in the tip region has changed 12˚.

The change of tip gap from 1 to 2 mm in the blade tip region had a 100˚ effect on the flow angle in the second stage, Fig. 14, which is substantial regarding the flow angle changes in the first stage.

The impact of tip clearance changes on outlet flow angle in the third stage is presented in Fig. 15. The tip clearance changes are highly effective on the outlet flow angle in the third stage and by changing the tip gap from 1 to 2 mm in this stage, a change of 150˚ is observed in the flow angle.

Figure 16 shows the leaked flow from the tip gap in the first, second and third rotors with 2mm tip clearance. It can be inferred that the leaked flow velocity from the blade tip of the third stage is much more than that of the first and second stages. As the rotational velocity of different stages is constant for all the stages, the reason for the difference in leaked flow velocity from the blade tip is the adverse pressure gradient in each compressor stage which is the greatest for the final stage.

One of the problems that provide stall condition is the improper angle which flow abandons the blade. It causes the flow entry to next rotor or stator with an unsuitable angle and it creates a condition to flow separation and then stall condition. By increasing tip clearance, the leakage flow is

increased and it affected to flow angle. Fig. 17 shows the outlet flow angle changes contour from the rotor stage. The black region is related to the changed angle due to the tip clearance of the rotor. The effect of tip clearance on the outlet angle can be seen as two spots on both sides of

passage related to the rotor. Concerning the first stage rotor, the tip clearance effect has not created the black region and this implies the lower sensitivity of the first stage rotor compared with the second and third stage rotors to the tip clearance.

8. CONCLUSION

After doing the experimental test of the compressor, the numerical analysis had done on the three stages of the compressor. Then numerical results were compared to experimental results. Then The performance curve of the compressor in the standard case was extracted without changes in the tip clearance by CFD analysis. By using numerical solutions, the performance diagrams of the compressor were obtained, showing good agreement with the experimental data diagram. The influence of tip clearance for different stages of the compressor was studied. The results indicate that the final stage of the compressor shows the highest sensitivity to the tip clearance changes. Unlike the presented results by Danisha *et al*., the effect of tip clearance is not influential on the choke flow rate for all stages and this tip gap change only effects the choke flow rate of the final stage of the compressor. The results show that for the tip clearance values of 1 and 2 mm in the first stage of the compressor, its efficiency drops by 1% and 2%, respectively. This amount of efficiency reduction in the second stage rotor for the tip clearance values of 1 to 2 mm is 2.5% and 6%, whereas they are 4% and 14% for the third stage rotor. Consequently, the effect of 1 mm tip clearance in the third stage has been higher than 2 mm tip clearance in the first stage, hence reducing the compressor efficiency to a greater degree.

REFERENCES

Bae, J. W., K. S. Breuer and C. S. Tan (2003). Active control of tip clearance flow in axial compressors. *ASME Turbo Expo 2003, collocated with the 2003 International Joint Power Generation Conference,* American Society of Mechanical Engineers 531-542.

Danisha, S. N., S. Qureshi, M. M. Imran, S. U. Din Khan, M. M. Sarfraz, A. El Leathyc, H. Al Ansaryc and M, Weid (2016). Effect of Tip Clearance and Rotor-Stator Axial Gap on the Efficiency of a Multistage Compressor. *Applied Thermal Engineering journal* 99, 988-995.

Day, I. J. (1993). Stall inception in axial flow compressors. *Journal of turbomachinery* 115, 1-9.

Day, I. J. (2015). Stall, Surge and 75 Years of Research. *Turbine Technical Conference and Exposition.* Montreal, Quebec, Canada, V006T47A001.

Day, I. J., T. Breuer, J. Escuret, M. Cherrett and A. Wilson (1997). Stall inception and the prospects for active control in four high speed compressors. *ASME 1997 International Gas Turbine and Aeroengine Congress and Exhibition*, American Society of Mechanical Engineers, V004T015A022V004T015A022.

Denton, J. D. (1993). Loss Mechanisms in Turbomachines. *Journal of Turbomachinery* 115, 621-656.

Hah, C., J. Bergner and H. P. Schiffer (2006). Short length-scale rotating stall inception in a transonic axial compressor: criteria and mechanisms. *ASME Turbo Expo: Power for land, sea, and air* 6, 61-70.

He, L. (1997). Computational study of rotating-stall inception in axial compressors. *Journal of Propulsion and Power* 13, 31-38.

Kim, J. H., K. J. Choi and K. Y. Kim (2013). Aerodynamic analysis and optimization of a transonic axial compressor with casing grooves to improve operating stability. *Aerospace Science and Technology* 29, 81-91.

Liou, B., G. An, X. Yu and Z. Zhang (2016). Experimental investigation of the effect of rotor tip gaps on 3D separating flows inside the stator of a highly loaded compressor stage. *Experimental Thermal and Fluid Science* 75, 96–107

Ramakrishna, P. V. and M. Govardhan (2009). Stall characteristics and tip clearance effects in forward swept axial compressor rotors. *Journal of Thermal Science* 18, 40-47.

Ren, X. and C. Gu (2016). A numerical study on the tip clearance in an axial transonic compressor rotor. *Applied Thermal Engineering* 103, 282-290.

Storer, J. A. and N. A. Cumpsty (1994). An approximate analysis and prediction method for tip clearance loss in axial compressors. *Journal of turbomachinery* 116, 648-656.

Vo, H. D., C. S. Tan and E. M. Greitzer (2008). Criteria for spike initiated rotating stall. *Journal of turbomachinery* 130, 011023.

Yamada, K., K. Funazaki and M. Furukawa (2007). The behavior of tip clearance flow at near-stall condition in a transonic axial compressor rotor. *ASME Turbo Expo 2007: Power for Land, Sea, and Air*, American Society of Mechanical Engineers 295-306.

Zhong, J., S. Han and P. Sun (2011). The influence of suction-side winglet on tip leakage flow in compressor cascade. *ASME 2011 Turbo Expo: Turbine Technical Conference and Exposition*. American Society of Mechanical Engineers 263-273.